Narrowing of band gap at source/drain contact scheme of nanoscale InAs–nMOS

A.H. Mohamed, R. Oxland, M. Aldegunde, S.P. Hepplestone, P.V. Sushko, K. Kalna

PII: S0038-1101(17)30738-4
DOI: https://doi.org/10.1016/j.sse.2018.01.006
Reference: SSE 7387

To appear in: *Solid-State Electronics*

Received Date: 25 October 2017
Accepted Date: 31 January 2018

Please cite this article as: Mohamed, A.H., Oxland, R., Aldegunde, M., Hepplestone, S.P., Sushko, P.V., Kalna, K., Narrowing of band gap at source/drain contact scheme of nanoscale InAs–nMOS, *Solid-State Electronics* (2018), doi: https://doi.org/10.1016/j.sse.2018.01.006

Narrowing of Band Gap at Source/Drain Contact Scheme of Nanoscale InAs–nMOS

A. H. Mohamed[1*], R. Oxland[2], M. Aldegunde[3], S. P. Hepplestone[4], P. V. Sushko[5], and K. Kalna[1]

[1] Nanoelectronic Devices Computational Group, College of Engineering, Swansea University, Swansea SA2 8PP
[2] TSMC R&D Europe B.V., 3001 Leuven, Belgium
[3] Warwick Centre for Predictive Modeling, School of Engineering, University of Warwick, Coventry CV4 7AL, UK
[4] Dept. of Physics and Astronomy, University of Exeter, School of Physics, Stocker Road, Exeter EX4 4QL, UK
[5] Physical & Computational Sciences Directorate, Pacific Northwest National Laboratory, Richland, WA 99352, USA
E-mail: a.h.mohamed.717812@swansea.ac.uk

Abstract. A multi-scale simulation study of Ni/InAs nano-scale contact aimed for the sub-14 nm technology is carried out to understand material and transport properties at a metal-semiconductor interface. The deposited Ni metal contact on an 11 nm thick InAs channel forms an 8.5 nm thick InAs leaving a 2.5 nm thick InAs channel on a *p*-type doped (1×10^{16} cm^{-3}) $AlAs_{0.47}Sb_{0.53}$ buffer. The density functional theory (DFT) calculations reveal a band gap narrowing in the InAs at the metal-semiconductor interface. The one-dimensional (1D) self-consistent Poisson-Schrödinger transport simulations using real-space material parameters extracted from the DFT calculations at the metal-semiconductor interface, exhibiting band gap narrowing, give a specific sheet resistance of R_{sh} = 90.9 **/sq** which is in a good agreement with an experimental value of 97 /sq.

Keywords: ab-initio, Band gap narrowing, MOSFETs, III–V semiconductors, 1D Poisson-Schrödinger, Schottky barrier height, Density Functional Theory (DFT).

1. Introduction

Metal-semiconductor contacts are essential components of many electronic devices [1]. Due to continuing scaling to nanometer dimensions, an accurate modeling of transport through metal-semiconductor contacts is the key to the development of novel nano-scale semiconductor devices [1, 2] such as the next generation of III–V based transistors [3]. The III-V compounds show a large potential as a high mobility channel material to replace the current silicon (*n*-type) transistor technology in CMOS [1, 2]. In addition to the high carrier mobility, they exhibit a high injection velocity resulting in reduced power dissipation at low voltage operations [3].

In this work, we present a multi-scale simulation study of a nano-scale contact combining density functional theory (DFT) calculations with solutions of 1D Poisson-Schrödinger (1DPS) equation aiming to understand a relation among contact resistance and band structure at the interface [4] relevant to the future of sub-10 nm technology [5, 6].

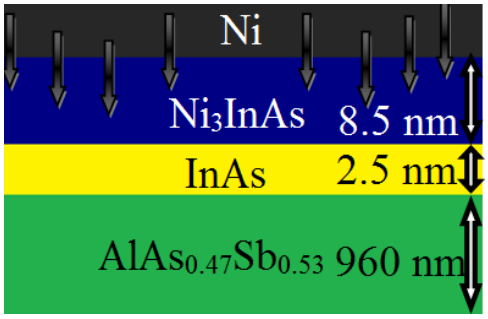

Fig. 1: Schematic of layers structure of the source/drain contact for a nano-scale InAs MOSFET. Structure has an 8.5 nm Ni_3InAs, 2.5 nm InAs, and $AlAs_{0.47}Sb_{0.53}$ buffer layers. The Ni_3InAs alloy is formed by Ni deposition on the 11 nm InAs layer. Black arrows indicate diffusion of Ni into InAs layer.

2. Ni contact for source/drain of III-V MOSFET

A description of the self-aligned device architecture of the heterostructure used in this paper is given in Fig. 1. In practice, the nano-scale contact under study is made of Ni metal interfacing an 11-nm thick InAs layer on *p*-type doped (1×10^{16} cm^{-3}) $AlAs_{0.47}Sb_{0.53}$ (960-nm) buffer. A thermal reaction between Ni and InAs results in the formation of an 8.5 nm thick Ni_3InAs layer [5] leaving only a 2.5 nm thick of InAs acting as a channel [5].

* Corresponding author
E-mail address: a.h.mohamed.717812@swansea.ac.uk (A. H. Mohamed).

3. Density functional theory calculation of the structure

In order to gain physical insight into carrier transport through the contact, we have employed 1DPS simulations using self-consistently [7] coupled Poisson-Schrödinger (PS) equations assuming a real-space dependent material parameters (band gap and affinity) obtained from *ab-initio* density functional theory (DFT) calculations [6]. The Ni_3InAs /InAs (100) interface was modelled as a periodic heterostructure shown in Fig. 2. The DFT calculations were performed to a large size of the unit cell (consisting of 1127 atoms) using the Perdew, Burke and Ernzerhof [8] functional and the projected augmented waves method [9] using the Vienna ab-initio simulation package (VASP) [10]. A 2×2×1 Monkhorst-Pack **k**-point set was used for the calculation with a cut-off of 500 eV. The density of states (DOS) for the semiconductor segment of the structure was projected on the atomic layers of In and As [4] to create the Layered Projected Density of States (LPDOS). LPDOS is divided into sub regions, along the direction perpendicular to the contact interface. Each sub region includes all atoms of one atomic plane as defined in the Ni_3InAs/InAs system in Fig. 2. Then, we calculate the LPDOS as a convolution of the DOS projected on each atom assigned to the corresponding sub region. As a sequence, the total energy of the system is set to the minimum with respect to the coordinates of all atoms and the cell parameters. Fig. 2 shows the geometric structure and density of states projected on atoms of each atomic plane in the InAs/Ni_3InAs (100) heterostructure [6].

4. 1D transport simulations

The source/drain (S/D) contact model used in the simulations was chosen to match the size and the composition of experimental structure made of an 11 nm thick InAs channel deposited on *p*-type $AlAs_{0.47}Sb_{0.53}$ buffer (doped to 1×10^{16} cm^{-3}) [5]. Then the

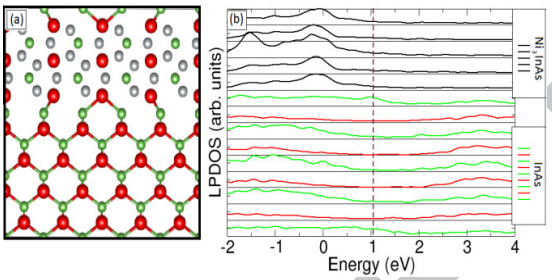

Fig. 2: (a) Atomic structure for Ni_3InAs/InAs (b) The layered projected density of states (LPDOS) for the Ni_3InAs/InAs interface calculated using VASP (PBE functional) from Ref. [6].

Ni deposited as a metal contact on S/D followed by thermal treatment to create an 8.5 nm thick Ni_3InAs alloy (behaves as a metal with a single energy level determined by the Fermi energy), leaving only a 2.5 nm thickness of un-doped InAs layers as a device channel (semiconductor), as it shown in Fig. 1.

Due to the well-known deficiencies of DFT, the LPDOS of InAs does not reproduce a true band gap. However, the LPDOS for the Ni_3InAs/InAs atoms has a band gap which follows the same trend as seen previously for the Mo/GaAs [4].

The thicknesses of the layers in the heterostructure, doping, energy band gaps, conduction band offset, mobility, electron effective masses, and permittivity are collected in Table I [11]. Note that the electron mobility in InAs has been obtained from Monte Carlo simulations as detailed in

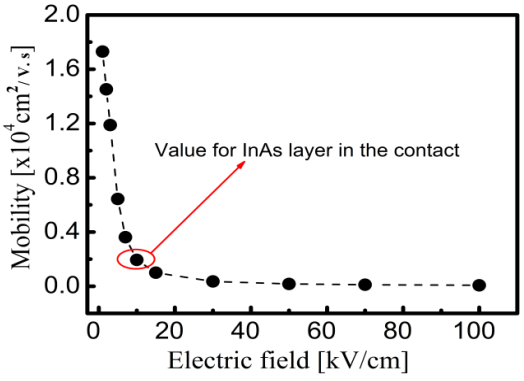

Fig. 3: Electron mobility vs. applied electric field in bulk InAs obtained from ensemble Monte Carlo simulations.

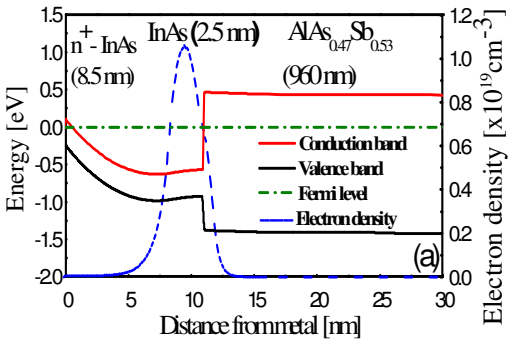

Fig. 4(b): Conduction and valence band profiles at equilibrium of the InAs (8.5nm)/InAs (2.5nm)/$AlAs_{0.47}Sb_{0.53}$ heterostructure assuming constant band gap for SBH of 0.11 eV.

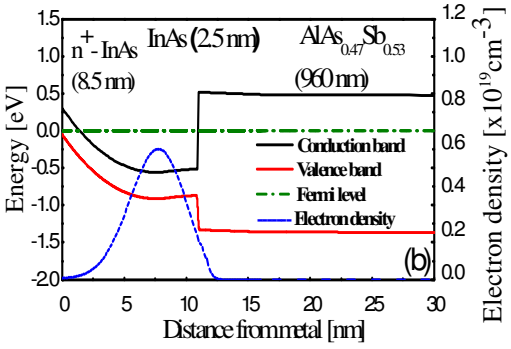

Fig. 4(b): Conduction and valence band profiles at equilibrium of the InAs (8.5nm)/InAs (2.5nm)/$AlAs_{0.47}Sb_{0.53}$ heterostructure assuming constant band gap for SBH of 0.30 eV.

the following.

Real-space dependent semiconductor material parameters assume that the equivalent change in a position of the edge of conduction and valence bands, energy gap, band offset occurs on the $Ni_3InAs/InAs$ interface as observed in the Mo/GaAs structure [4].

The band structure assumes that only the lowest valleys in semiconductors (InAs and $AlAs_{0.47}Sb_{0.53}$) are active in the transport through the contact which is reasonable approximation in this heavily doped structure [6]. In order to determine the mobility of InAs used then in the 1DPS simulations, we estimate the electric field first, assuming a 1 V bias applied across the contact [12]. Electric field F can be calculated as $F = V/t$ [12], where t is the thickness of a structure (11 nm InAs and 960 nm $AlAs_{0.47}Sb_{0.53}$) to get:

$$F = \frac{V}{t_{(InAs+AlAsSb)}} = \frac{1\,V}{971\,nm} \approx 10\ kV/cm$$The

TABLE I: InAs, AND $AlAs_{0.47}Sb_{0.53}$ MATERIAL PARAMETERS USED IN MODELLING OF THE InAs/$AlAs_{0.47}Sb_{0.53}$ CONTACT.

Material Thickness [nm]	*n*-type doping [cm^{-3}]	*p*-type doping [cm^{-3}]	E_G [eV]	ΔE_C [eV]	μ [cm^2/Vs]	m_e [m_0]	ε_r [ε_0]
8.5 (InAs)	3×10^{19}	1×10^{14}	0.354	-0.71	200	0.023	15.50
2.5 (InAs)	1×10^{16}	1×10^{14}	0.354	-0.71	1960	0.023	15.50
960 ($AlAs_{0.47}Sb_{0.53}$)	1×10^{14}	1×10^{16}	1.846	0.315	1350	0.088	10.95

electron mobility in InAs (intrinsic) plotted in Fig. 3 as a function of applied electric field has been obtained from bulk ensemble Monte Carlo simulations [13]. Details of these Monte Carlo simulations can be found in Refs. [14,15]. Fig. 3 shows that, at an electric field of 10kV/cm, the intrinsic electron mobility of *n*-type InAs doped to 1×10^{16} cm^{-3} (nearly intrinsic) is 1960 cm^2/Vs, and 200 cm^2/Vs when *n*-type doped to 3×10^{19} cm^{-3} [16] as collected in Table I. Finally, the electron mobility of *p*-type $AlAs_{0.47}Sb_{0.53}$ (doping concentration 1×10^{16}) used in the 1DPS is 1350 cm^2/Vs and is based on the experimental data taking into consideration the material composition of $AlAs_{0.47}Sb_{0.53}$ and carrier concentration [17].

Fig. 4 shows the conduction band, valence bands and Fermi level overlapped with electron density from the 1DPS solutions. We assume a bulk metal work function of Ni (5.01 eV) and calculate Schottky barrier height (SBH) as a potential difference between the work function and electron affinity. For the metal work function (5.01 eV) and affinity (4.9 eV) [6], the SBH was extracted as 0.11 eV. The work function dramatically affects the transport at the interface and the sheet resistance value was calculated (165 Ω/sq). When the metal work function takes a value of 4.79 eV [6], the SBH increases from 0.11 eV to 0.30 eV.

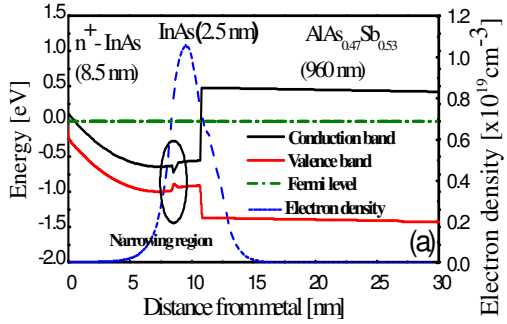

Fig. 5(a): Conduction and valence band profiles for Ni/InAs (8.5nm)/InAs (2.5nm)/$AlAs_{0.47}Sb_{0.53}$ heterostructure assuming the band gap narrowing and a SBH of 0.11 eV at equilibrium. Band gap narrowing of InAs at the interface from the DFT is: ΔE_G (0.2nm) = 0.154 eV, ΔE_G (0.4nm) = 0.204 eV, ΔE_G (0.6nm) = 0.254 eV, ΔE_G (0.8nm) = 0.304eV, ΔE_G (1.0nm) = 0.354 eV.

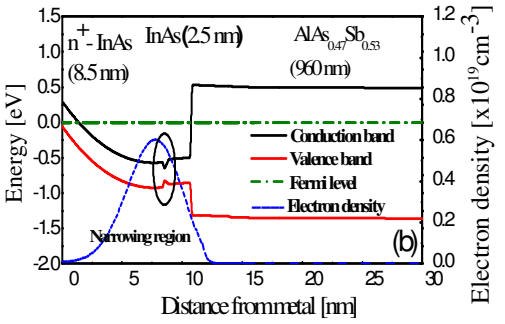

Fig. 5(b): Conduction and valence band profiles at equilibrium of the Ni/InAs (8.5nm)/InAs (2.5nm)/$AlAs_{0.47}Sb_{0.53}$ heterostructure assuming constant band-gap for a SBH of 0.30 eV. Band gap narrowing of InAs at the interface follows the same steps as in the caption of Fig. 5(a).

Due to the increase in the SBH, the sheet resistance increases to 203.7 Ω/sq. This value is approximately around 110% larger than the experimentally measured because electrons have to tunnel through a larger potential barrier [18]. In a comparison, the sheet resistance at a metal work function of 5.01 eV is larger by about 70% than the experimentally observed.

5. Band Gap Narrowing

The band gap narrowing in InAs semiconductor is modelled as follows. The coordinates for the band gap narrowing in InAs layer (see the caption of Fig. 5a) are obtained from DFT calculations [4] of a nanoscale Mo/GaAs contact assuming the same narrowing proportional to the band gap of InAs. The region of InAs at the metal-semiconductor interface is divided into 5 equal regions. For every node of the 1D mesh, we then computed the distance to the metal contact and adjust the values of InAs (electron effective mass, the band gap and the electron affinity) using the calculated position dependent values [4] as shown in the caption of Fig. 5. The band gap narrowing of the heavily *n*-doped is assumed to be the same as the band gap narrowing of the heavily *n*-doped GaAs band gap in Ref. [4]. The electron effective mass dependent on the real-space position are transferred from the DFT calculations into the 1DPS simulation [8]. Figure 5 shows conduction and valence bands overlapped with electron density of the effect of band gap narrowing for two values of Schottky barrier height (0.1 eV, 0.3 eV). We can see that the electron wave function penetration is substantially reduced due to change in the shape of Schottky barrier which becomes 'thinner' for electrons to tunnel through as a results, sheet resistance has been decreased from 90.9 Ω/sq to 63.85 Ω/sq (by about 42%) [5].

Figure 6 shows the variation in a sheet resistance with a metal work function obtained from 1DPS simulations assuming a constant band gap (band gap without narrowing) in the InAs layer (black circles) and assuming the band gap narrowing (red square). Only when the band gap narrowing is taken into account the simulations give an agreement with the experimental value (green diamond). Hence, with the band gap narrowing, our results given R_{sh} of 90.9 Ω/sq, which is in a good agreement with the measured result of 97Ω/sq [5].

If the band gap narrowing is not included, the abrupt metal semiconductor interface results in a lower tunneling probability which increases the sheet resistance to 203.7 Ω/sq. The results obtained for different combinations are collected in Table II.

TABLE II: SHEET RESISTANCE OF A NANOSCALE METAL CONTACT FOR SEVERAL COMBINATIONS OF PARAMETERS.

Affinity/ Band gap	Effective mass	Schottky barrier height [eV]	Sheet Resistance (Ω/sq)
Constant	Constant	0.11	165
Constant	Constant	0.30	203.7
Narrowing	Position dependent	0.11	63.85
Narrowing	Position dependent	0.30	90.9

When we take into account the band gap electron effective mass, the sheet resistance decreases. This is caused by the dependence of the tunnelling (a penetration of electron wave function though a barrier) probability on the barrier shape, not only on the SBH, which, in turn, is determined by the position dependent material parameters. Notably, the barrier becomes narrower which leads to an increase in the current flow through the contact [18].

6. Conclusion

We have developed a multi-scale model for carrier transport in metal-semiconductor contacts using first principle calculations (DFT) which provide input for the 1D self-consistent PS simulations. We have demonstrated that the transport properties, in particular, the sheet resistance can be calculated more accurately within multi-scale model than when using a method of SBH and constant semiconductor band gap and affinity.

We have employed this multi-scale modeling approach to study a sheet resistance of the S/D contacts aimed for future III–V *n*-MOS in order to give insight into the transport between the interfaces through a nanoscale metal-semiconductor contact. We have shown that the inclusion of a realistic band structure at the interface results in a larger tunneling current than would have been obtained from Schottky contact model while assuming a bulk work function of Ni (5.01 eV). This decreases the sheet resistance of the contact to 90.9 Ω/sq which is in a very good agreement with the experimentally measured value of 97 Ω/sq [5]. This agreement reveals that the band gap narrowing plays an essential role in determination of the sheet resistance of a nanoscale metal contact.

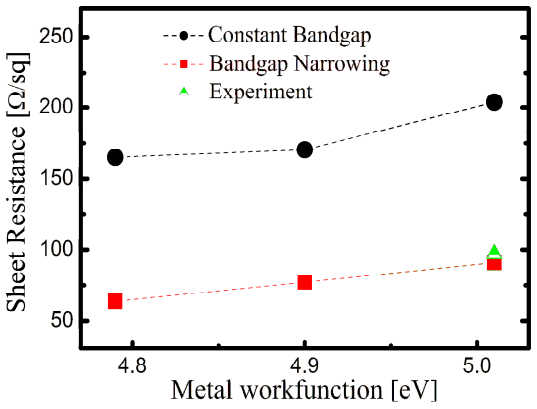

Fig. 6: Sheet resistance for InAs(8.5 nm)/InAs(2.5 nm)/$AlAs_{0.47}Sb_{0.53}$(960 nm) contact heterostructure as a function of metal work function (Ni) comparing simulations using the same band gap in whole InAs and those when the band gap narrowing towards metal-semiconductor interface is accounted for the experimental value of sheet resistance [4] is shown by green triangle.

References

[1] International technology Roadmap for semiconductors, 2011. [Online]. http://public.itrs.net.

[2] K. Takei, H. Fang, S. B. Kumar, Q. Gao, M. Madsen, H. S. Kim, C. H. Liu, Y. L. Chueh, R. Kapadia, S. Chuang, P. W. Leu, K. Ganapathi, E. Plis, and S. Krishna, "Quantum confinement effects in nanoscale-thickness InAs membranes," *Nano Lett.*, vol. 11, no. 11, pp. 5008-5012, Nov. 2010.

[3] K. Kalna, N. Seoane, A. J. Loureiro, I. G. Thayne, and A. Asenov, "Benchmarking of scaled InGaAs implant-free nano MOSFETs," *IEEE Trans. Electron Devices*, vol. 55, no. 9, pp. 2297-2306, Sept. 2008.

[4] M. Aldegunde, S. P. Hepplestone, P. V. Sushko, and K. Kalna, "Multi-scale simulations of a Mo/n+–GaAs Schottky contact for nano-scale III–V MOSFETs," *Semicond. Sci. Tech.,* vol. 29, no. 5, art 54003, Apr. 2014.

[5] R. Oxland, S. W. Chang, Li. X. Wang, S. W. Radhakrishnan, G. W. Priyantha, and Y. C. Sun, "An Ultralow-resistance ultra-shallow metallic source/drain contact

scheme for III–V NMOS," *IEEE Electron Device Lett*., vol. 33, no. 4, pp. 501-503, Feb. 2012.

[6] G. Schusteritsch, S. P. Hepplestone, and C. J. Pickard, "First-principles structure determination of interface materials: The Ni_xInAs nickelides," *Phys. Rev. B*, vol. 92, no. 5, pp. 054105, 2015.

[7] I.-H. Tan, G. L. Snider, L. D. Chang, and E. L. Hu, "A self-consistent solution of Schrödinger–Poisson equations using a nonuniform mesh," *J. Appl. Phys.,* vol. 68, no. 8, pp. 4071-4076, Dec. 1990.

[8] J. P. Perdew, K. Burke, and M. Ernzerhof, "Generalized gradient approximation made simple," *Phys. Rev. Lett*., vol. 77, pp. 3865-3868, 1996.

[9] P. E. Blöchl, "Projector augmented-wave method," *Phys. Rev. B*, vol. 50, pp. 17953-17979, 1994.

[10] G. Kresse and J. Furthmüller, "Ab-initio free energy calculations on the polymorphs of iron at core conditions," *Phys. Rev. B*, vol. 54, pp. 11169-11186, 1996.

[11] Physical Properties of Semiconductors, Ioffe Inst. [Online]: http://www.ioffe.ru.

[12] K. Kalna, S. Roy, A. Asenov, K. Elgaid, and I. Thayne, "Scaling of pseudomorphic high electron mobility transistors to decanano dimensions," *Solid State Electron*., vol. 46, no. 5, pp. 631-638, May. 2002.

[13] A. Islam, B. Benbakhti, and K. Kalna, "Monte Carlo study of ultimate channel scaling in Si and $In_{0.3}Ga_{0.7}As$ bulk MOSFETs," *IEEE Trans. Nanotechnol*., vol. 10, no. 6, pp. 1424-1432, Nov. 2011.

[14] K. Kalna, S. Roy, A. Asenov, K. Elgaid and I. Thayne, "Scaling of pseudomorphic high electron mobility transistors to decanano dimensions", *Solid-St. Electron.* vol. 46, no. 5, pp. 631-638, May 2002.

[15] K. Kalna and A. Asenov, "Nonequilibrium transport in scaled high electron mobility transistors", *Semicond. Sci. Technol.*, vol. 17, no. 6, pp. 579-584, May 2002.

[16] B. Benbakhti, A. Martinez, K. Kalna, Hellings, G. Eneman, K. De Meyer, and M. Meuris, "Simulation Study of Performance for a 20-nm Gate Length $In_{0.53}Ga_{0.47}As$ Implant Free Quantum Well MOSFET," *IEEE Trans Nanotechnol.*, vol. 11, no. 4, pp. 808-817, July 2012.

[17] Ł. Piskorski and R.P. Sarzała, "Material parameters of antimonides and amorphous materials for modelling the mid-infrared lasers," *Opt. Appl*., vol. 46, no. 2, pp. 227-240, 2016.

[18] S. E. Mohney, Y. Wang, M. A. Cabassi, K. K. Lew, S. Dey, J. M. Redwing, and T. S. Mayer, "Measuring the specific contact resistance of contacts to semiconductor nanowires," *Solid-State Electron.,* vol. 49, no. 2, pp. 227-232, 2005.

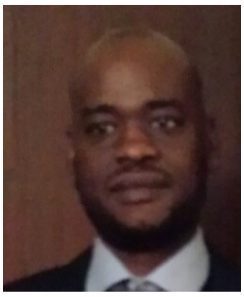

Alnazer Hamed Mohamed received the MSc degree in Physics science from University of Khartoum, Khartoum in 2011. I'm currently working toward the Ph.D. degree in electronic and electrical engineering at Swansea University, UK. My current research interests are included electronic transport in modern-nanoscale and Metal-Semiconductor Contacts devices and their modelling and simulation using Schrodinger Poisson equations and other different approach.